Langmuir

Letter

pubs.acs.org/Langmuir

Monitoring Picoliter Sessile Microdroplet Dynamics Shows That Size Does Not Matter

Isaac Rodríguez-Ruiz,[†] Zoubida Hammadi,[‡] Romain Grossier,[‡] Jaime Gómez-Morales,[†] and Stéphane Veesler*[,‡]

[†]Laboratorio de Estudios Cristalográficos, IACT (CSIC-UGR), Avda. de las Palmeras, 4, 18100 Armilla, Granada, Spain

[‡]CINaM-CNRS, Aix-Marseille Université, Campus de Luminy, F-13288 Marseille, France

Supporting Information

ABSTRACT: We monitor the dissolution of arrayed picoliter-size sessile microdroplets of the aqueous phase in oil, generated using a recently developed fluidic device. Initial pinning of the microdroplet perimeter leads to a nearly constant contact diameter, thus contraction proceeds via microdroplet (micrometer-diameter) height and contact angle reductions. This confirms that picoliter microdroplets contraction or dissolution due to the selective diffusion of water in oil has comparable dynamics with microliter droplet evaporation in air. We observe a constant microdroplet dissolution rate in different aqueous solutions. The application of this simple model to solvent-diffusion-driven crystallization experiments in confined volumes, for instance, would allow us to determine precisely the concentration in the microdroplet during an experiment and particularly at nucleation.

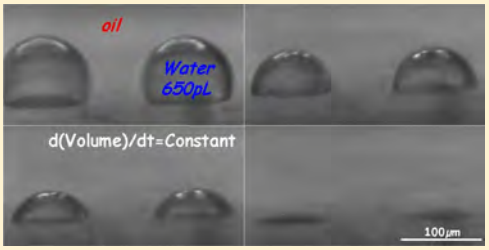

INTRODUCTION

Numerous applications involve reducing the droplet volume with time: drying of colloidal suspensions,[1] drying of human blood drops for diagnostic purposes,[2] coffee ring deposition on solid surfaces,[3] efficacy and efficiency of pesticide application,[4] meteorology and air-conditioning,[5] nanoscale pipetting for confined chemistry,[6] detection of molecules and biomarkers below picomolar concentration,[7] deterioration of building materials[8,9] (due to salt crystallization in the pores), inkjet-based direct writing technology,[10] crystallization of proteins,[11] and crystallization in confined environments.[12,13] Understanding how droplet volume can be reduced means looking at the dynamics of droplet evaporation, drying, dissolution, or contraction for geometries ranging from aerosol to sessile and sizes ranging from millimeter to micrometer. Sessile droplet evolution can be characterized by monitoring over time the contact angle of the droplet with the substrate, the droplet height, and the contact diameter. Thus, the evaporation of a sessile droplet in the microliter range is known to proceed through different modes: constant contact angle, constant contact area, and mixed mode, depending on the surface roughness and chemical nature, atmospheric conditions, and droplet size.[14−17] Although it is of interest to consider picoliter droplets (micrometer diameter) to check the model validity on this scale, there are few references to this in the literature.[18−21] Most experiments are performed with microliter droplets (millimeter diameter) mainly due to the rapid evaporation of such small microdroplets, rendering quantitative measurements difficult. In this context, it has proven challenging to perform quantitative monitoring of droplet dynamics in the micrometer range: the smaller the droplet, the faster the dynamics. Although fast imaging may have potential, there are still limitations regarding the accuracy of the measurement of the first instants of these droplet dynamics. In this letter, we use the terms microdroplets for droplets in the micrometer range and droplets for droplets in the millimeter range.

Recently, we presented a simply constructed and easy-to-use fluidic device that generates arrayed aqueous phase microdroplets under oil (sessile geometry), with volumes ranging from nanoliters to femtoliters, without surfactant.[22] In subnanoliter experiments performed with this fluidic device, we observed the contraction of NaCl microdroplets[23] resulting from the selective diffusion of water in oil,[24] which acts as a buffer to slow down the diffusion rate. This process generates an increment of solute concentration and thus supersaturation, ensuring crystallization. This application illustrates the potential of this technology in the field of particle generation, where small-volume systems have promising properties.[12,13] Microdroplets were observed under an inverted optical microscope, and the solute concentration was qualitatively monitored through the evolution of the optical contrast between the droplet and the continuous phase. For a more precise and quantitative determination of the solute concentration during the diffusion process, it should be possible to monitor the droplet volume. This was performed, for instance, by image analysis of dispersed aqueous salt solutions in silicone oil[24,25] but not for sessile microdroplets.

Here, to measure the solute concentration, we perform experiments in which the contraction of sessile microdroplets of the aqueous phase into oil is observed using an optical microscope. The contact angle of the microdroplet with the

Received: July 18, 2013
Revised: September 25, 2013
Published: September 26, 2013

substrate, microdroplet height, and contact diameter are monitored during the diffusion of water into oil, and using the simple trigonometry presented in the Supporting Information, microdroplet volumes are computed. We observe a constant microdroplet dissolution rate whatever the microdroplet composition. In this letter, we show that this microdroplet contraction or dissolution due to the selective diffusion of water in oil is equivalent to the evaporation of a droplet in air in stationary diffusion-controlled evaporation with local equilibrium at the drop interface.[16]

EXPERIMENTAL SECTION

Microdroplets are generated[22] under an optical microscope (Zeiss Axio Observer D1) by a microinjector (Femtojet, Eppendorf) on a plastic coverslip (22 × 22 mm^2 SPI) covered with approximately 100 μL of paraffin oil (HR3-421) and inserted into a homemade plastic cell with vertical walls for side observation using an optical microscope. The cell is then transferred and observed under a side-view microscope (Olympus BXFM focusing module equipped with a homemade holder) (Figure 1). Here the solution is a 2.71 M NaCl aqueous solution with half the solubility of NaCl in water at 20 °C;[26] see the Supporting Information for solution preparation.

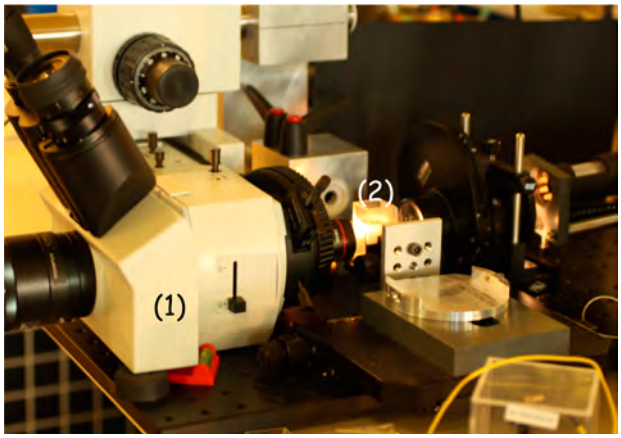

Figure 1. Image of the experimental setup for side observation: (1) microscope and (2) plastic cell.

Figure 2 presents top and side views of a part of an array of 2.71 M NaCl microdroplets in oil. In a previous paper, we showed the

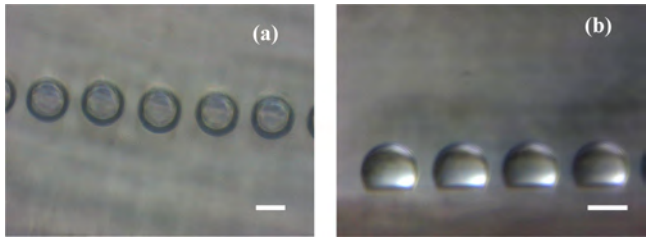

Figure 2. (a) Top view and (b) side view of 2.71 M NaCl microdroplets (151 pL) in oil. The scale bar represents 50 μm.

monodispersity of the droplet size at the pixel resolution.[22] For instance, the volume of the four microdroplets in Figure 2b is 151 ± 7pL. (Details of the calculation are given in the Supporting Information.)

RESULTS AND DISCUSSION

The sequence in Figure 3 presents the 2.71 M NaCl microdroplet contraction by the diffusion of water into oil. During contraction, the solution becomes increasingly concentrated. At the end of the process, when the concentration reached instability, the microdroplets collapse because of the nucleation and growth of a single crystal per microdroplet in accordance with our theoretical prediction.[27] One example of an application this phenomenon is its use to deposit a solute in a confined region.[7]

In practice, because of the microdroplet size, we can assume that there is no shape distortion due to gravity; this is confirmed by the value of the Bond number of 3.7×10^{-6} for a microdroplet of 100 μm diameter.[28] Thus, microdroplet profiles can be fitted to a segment of a circle.[14,18] Thus, the contact angle of the microdroplet with the substrate, microdroplet height, and contact diameter can be easily extracted from this experiment (Figure 4 and Supporting Information).

Contact Angle (Figure 4a). The evaporation of a sessile droplet is known to proceed through different modes as mentioned above. Figure 4a shows a continuous decrease in the contact angle, θ. The initial contact angle can be identified as an advancing angle (θ_A), which decreases until it reaches the receding angle (θ_R), thus

$$\theta_A > \theta > \theta_R \tag{1}$$

This decrease is the "stage II" described by Bourgès-Monnier and Shanahan,[15] where the height and contact angle decrease while the contact diameter remains constant (also known in the literature as the constant contact diameter mode or the CCD mode). At the end of stage II, the contact angle is θ_R and should remain constant, although this is not observed here because nucleation has already occurred (Figure 3f–i).

Height and Contact Diameter (Figure 4b). The evolution of these parameters confirms that the process is in stage II. An initial pinning of the perimeter leads to a nearly constant contact diameter (respectively area), thus contraction proceeds via microdroplet height and contact angle reductions.[18] These results confirm that the evaporation of picoliter microdroplets is comparable to that of microliter droplets. Moreover, the rapid decrease in θ in the first stage due to rapid evaporation in air observed by Taylor et al.[18] is not observed because the oil acts as a buffer. As stated by Duncan and Needham,[29] compared to pure gas–liquid systems (air–water), pure liquid–liquid (oil–water) systems have higher densities (~1000×), lower diffusion constants (~10×), and lower solubility-limit concentrations (~100×); therefore, the dissolution lifetime can vary from seconds to hours. For instance, in previous experiments presented by Furuta,[19] the evaporation of a 800 pL droplet in air takes about 8 s, whereas here evaporation takes several hours.

Volume Contraction (Figure 5). Figure 5 presents the evolution of NaCl-, water-, Na_2CO_3- and $CaCl_2$-microdroplet volumes with time; lines are linear fits of the data corresponding to a constant microdroplet dissolution rate (eq 2)

$$\frac{V}{V_0} = (1 - \alpha \times t) \tag{2}$$

with V_0 and V are the initial and time t microdroplet volumes, respectively, and α is the normalized dissolution rate; α is a linear function of the saturation fraction of water in oil.[29] A semilog plot is used in Figure 5b,d to illustrate the apparent final acceleration in the evaporation, which is not due to an increase in the evaporation rate but rather to the fact that there is less matter to evaporate.

The dissolution rate of a water microdroplet into an infinite medium is known to be constant. In our experiments, water microdroplets of 64.6(±1.2) pL are formed in an immiscible medium having a volume of ~100 μL (6 orders of magnitude

dx.doi.org/10.1021/la402735k | Langmuir 2013, 29, 12628–12632

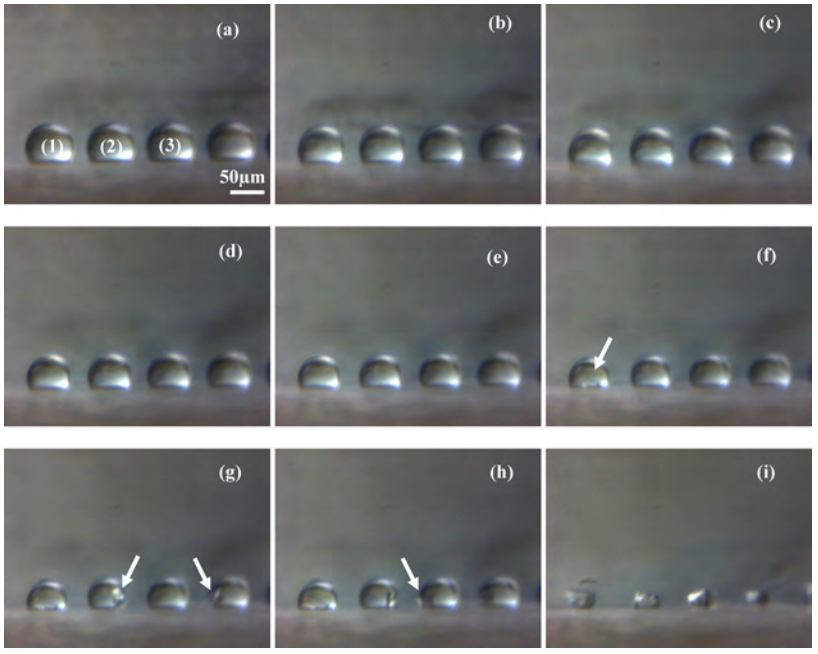

Figure 3. Time sequence showing the side view of 2.71 M NaCl microdroplet (151 pL) contraction in oil: (a) $t = 0$ min, (b) $t = 60.05$ min, (c) $t = 130.12$ min, (d) $t = 190.18$ min, (e) $t = 260.25$ min, (f) $t = 330.32$ min (g) $t = 360.32$ min, (h) $t = 380.32$ min, and (i) $t = 740.31$ min. Arrows in f–h show crystals. See the Supporting Information for a movie of this process.

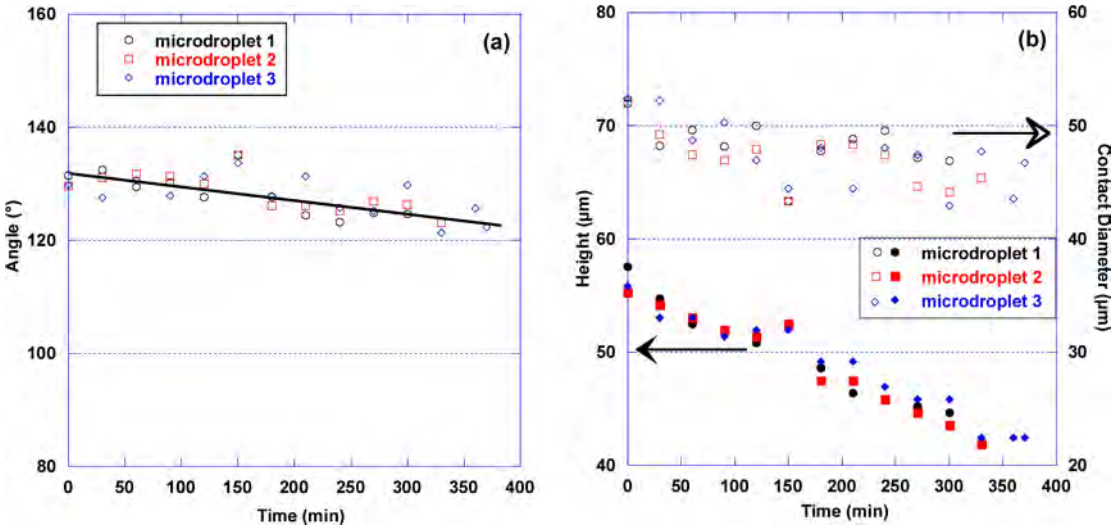

Figure 4. (a) Contact angle of the microdroplets with the substrate and (b) microdroplet height and contact diameter. The line is a guide to the eyes, and microdroplets are from Figure 3

larger than that of the microdroplets), which means that the water droplet is in an effectively infinitely dilution regime, as confirmed by the constant value of α obtained in our experiments in pure water (Figure 5a). Moreover, when a salt is added to water the rate of solvent dissolution will be constant for a dilute solution if the activity of water is not greatly affected by the presence of salt. In their paper, Talreja et al.[30] assumed a constant evaporation rate for protein and salt solutions until $V/V_0 = 0.15$. In our experiments with 2.71 M NaCl solutions (Figure 5a,b), the dissolution rate is constant until nucleation occurs for $V/V_0 > 0.4$, in agreement with Talreja et al. Moreover, the dissolution rate is also constant for Na_2CO_3- and $CaCl_2$-microdroplet dissolution.

It is well known that a constant total evaporation rate and a volume decreasing linearly with time at constant contact diameter are observed for the evaporation of a sessile droplet in quiescent open air under partial wetting if the contact line is pinned.[3,14,16,31] This is the case in our experiments. Therefore, the overall behavior of microdroplet dissolution is identical to that of stationary diffusion-controlled evaporation with local equilibrium at the drop interface.[16] Note that at the very end of the process, for $V/V_0 < 0.1$ in the case of water microdroplets (Figure 5a,b and Figure S2 in Supporting Information), this simple model no longer works.

Finally, we tested the modified model of Picknett and Bexon[14] by McHale et al.[32] for the CCD mode with diffusion-controlled evaporation (eq 20 in ref 32 and the Supporting Information). This model, valid only for $\theta \geq 90°$ as in our experiments, gives the diffusion constant–concentration difference product estimation in agreement with the literature (Supporting Information).

dx.doi.org/10.1021/la402735k | *Langmuir* 2013, 29, 12628–12632

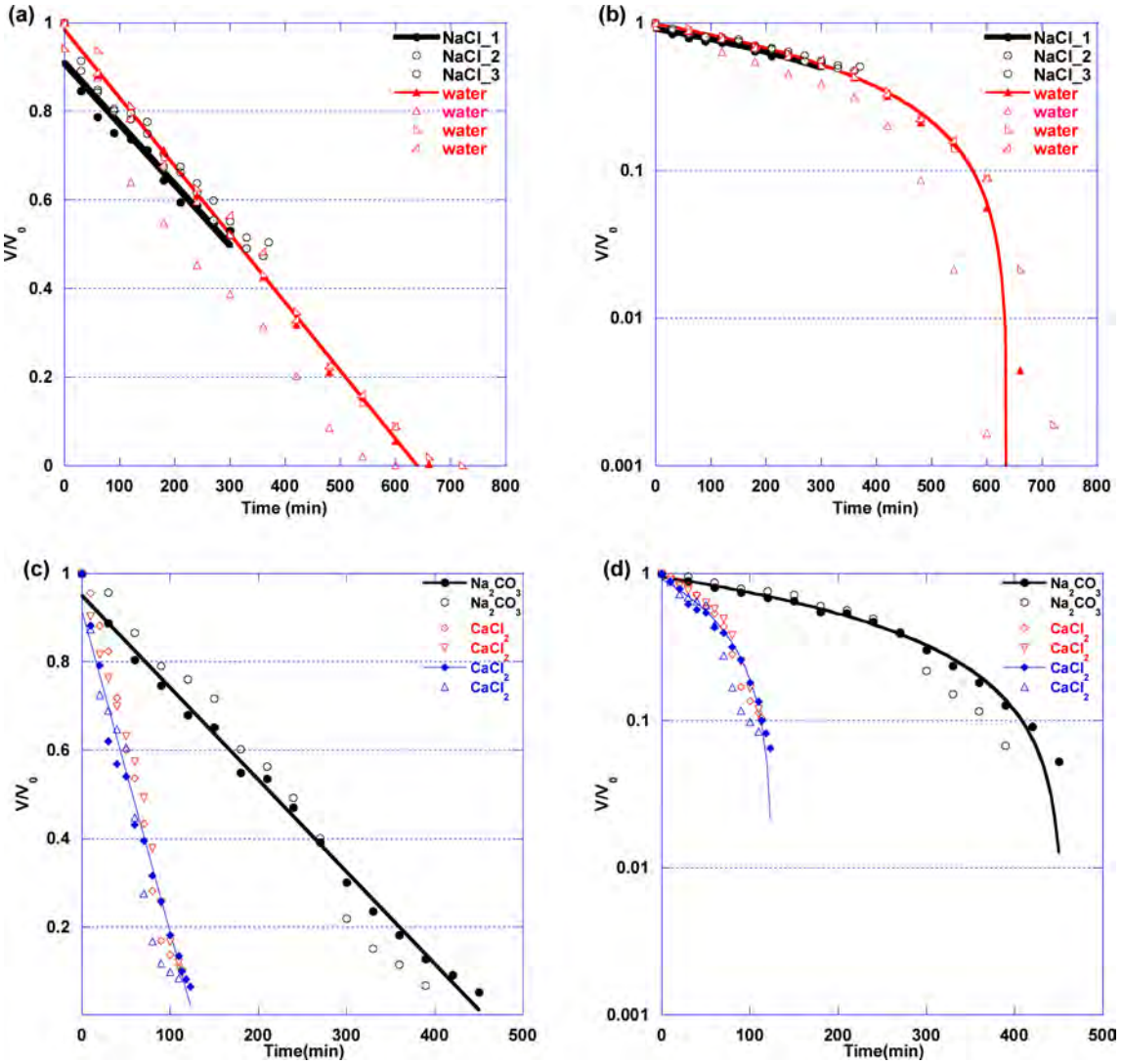

Figure 5. Volume contraction on (a) linear and (b) semilog plots for the 2.71 M NaCl and water microdroplets with initial volumes of 151 (±7) and 64.6(±1.2) pL, respectively and on (c) linear and (d) semilog plots for 60 mM Na_2CO_3 and $CaCl_2$ microdroplets with initial volumes of 655(±24) and 42.2(±5.5) pL, respectively. NaCl microdroplets are from Figure 3; lines are linear fits to the data.

In conclusion, we present experiments in which the contraction of sessile microdroplets of the aqueous phase in oil is monitored using a recently developed[22] fluidic device that generates arrayed aqueous-phase microdroplets in oil. Initial pinning of the microdroplet perimeter leads to a nearly constant contact diameter, thus contraction proceeds via microdroplet height and contact angle reductions. This confirms the process to be the stage II described by Bourgès-Monnier and Shanahan[15] for the evaporation of a sessile droplet corresponding to stationary diffusion-controlled evaporation with local equilibrium at the drop interface.[16] Thus, microdroplets (micrometer diameter) behave like droplets. We observed a constant dissolution rate of the microdroplet for pure water and in different salts. The application of this simple model to solvent-diffusion-driven crystallization experiments in confined volumes, for instance, would allow us to determine precisely the concentration in the microdroplet during an experiment and particularly at nucleation.

■ ASSOCIATED CONTENT

Ⓢ Supporting Information

Reagents and solutions; graph of the contact angle, height, and contact diameter for water microdroplets; time sequence of volume contraction for water microdroplets; test of constant contact radius mode with diffusion-controlled evaporation and computation of the contact angle of the microdroplet with the substrate; and microdroplet height, contact diameter, and microdroplet volumes. Video showing a side view of 2.71 M NaCl microdroplet contraction in oil. This material is available free of charge via the Internet at http://pubs.acs.org.

■ AUTHOR INFORMATION

Corresponding Author

*Phone: 336 6292 2866. Fax: 334 9141 8916. E-mail: veesler@cinam.univ-mrs.fr.

Notes

The authors declare no competing financial interest.

dx.doi.org/10.1021/la402735k | *Langmuir* 2013, 29, 12628−12632

■ ACKNOWLEDGMENTS

This work was carried out within the framework of project MAT2011-28543 (Spanish MINECO). J.G.-M. and I.R.-R. belong to the research team "Factoría de Cristalización" (Consolider Ingenio 2010) of the Spanish Ministerio de Ciencia e Innovación. I.R.-R. also acknowledges CSIC for his JAE-Pre contract cofunded by the European Social Fund. We thank Professor Juan Manuel García-Ruiz for supporting I.R.-R. and encouraging him to perform this research. We thank M. Sweetko for the English revision and ANR2010 BLAN 031102 "Smart Us" for financial support.

■ REFERENCES

(1) Parisse, F.; Allain, C. Drying of Colloidal Suspension Droplets: Experimental Study and Profile Renormalization. *Langmuir* **1997**, *13*, 3598−3602.
(2) Brutin, D.; Sobac, B.; Loquet, B.; Sampol, J. Pattern Formation in Drying Drops of Blood. *J. Fluid Mech.* **2011**, *667*, 85−95.
(3) Deegan, R. D.; Bakajin, O.; Dupont, T. F.; Huber, G.; Nagel, S. R.; Witten, T. A. Capillary Flow As the Cause of Ring Stains from Dried Liquid Drops. *Nature* **1997**, *389*, 827−829.
(4) Yu, Y.; Zhu, H.; Frantz, J. M.; Reding, M. E.; Chan, K. C.; Ozkan, H. E. Evaporation and Coverage Area of Pesticide Droplets on Hairy and Waxy Leaves. *Biosyst. Eng.* **2009**, *104*, 324−334.
(5) Houghton, H. G. A Study of the Evaporation of Small Water Drops. *Physics* **1933**, *4*, 419−424.
(6) Rodolfa, K. T.; Bruckbauer, A.; Zhou, D.; Schevchuk, A. I.; Korchev, Y. E.; Klenerman, D. Nanoscale Pipetting for Controlled Chemistry in Small Arrayed Water Droplets Using a Double-Barrel Pipet. *Nano Lett.* **2006**, *6*, 252−257.
(7) De Angelis, F.; Gentile, F.; Mecarini, F.; Das, G.; Moretti, M.; Candeloro, P.; Coluccio, M. L.; Cojoc, G.; Accardo, A.; Liberale, C.; Zaccaria, R. P.; Perozziello, G.; Tirinato, L.; Toma, A.; Cuda, G.; Cingolani, R.; Di Fabrizio, E. Breaking the Diffusion Limit with Super-Hydrophobic Delivery of Molecules to Plasmonic Nanofocusing SERS Structures. *Nat. Photon.* **2011**, *5*, 682−687.
(8) Winkler, E. M.; Singer, P. C. Crystallization Pressure of Salts in Stone and Concrete. *Geol. Soc. Am. Bull.* **1972**, *83*, 3509−3514.
(9) Shahidzadeh-Bonn, N.; Desarnaud, J.; Bertrand, F.; Chateau, X.; Bonn, D. Damage in Porous Media Due to Salt Crystallization. *Phys. Rev. E* **2010**, *81*, 066110.
(10) Hon, K. K. B.; Li, L.; Hutchings, I. M. Direct Writing Technology–Advances and Developments. *CIRP Ann.* **2008**, *57*, 601−620.
(11) Ducruix, A.; Giégé, R. *Crystallization of Nucleic Acids and Proteins: A Practical Approach*, 2nd ed.; Oxford University Press: Oxford, U.K., 1999; p 460.
(12) Lee, A. Y.; Lee, I. S.; Dette, S. S.; Boerner, J.; Myerson, A. S. Crystallization on Confined Engineered Surfaces: A Method to Control Crystal Size and Generate Different Polymorphs. *J. Am. Chem. Soc.* **2005**, *127*, 14982−14983.
(13) Grossier, R.; Hammadi, Z.; Morin, R.; Veesler, S. Predictive Nucleation of Crystals in Small Volumes and Its Consequences. *Phys. Rev. Lett.* **2011**, *107*, 025504.
(14) Picknett, R. G.; Bexon, R. The Evaporation of Sessile or Pendant Drops in Still Air. *J. Colloid Interface Sci.* **1977**, *61*, 336−350.
(15) Bourges-Monnier, C.; Shanahan, M. E. R. Influence of Evaporation on Contact Angle. *Langmuir* **1995**, *11*, 2820−2829.
(16) Cazabat, A.-M.; Guena, G. Evaporation of Macroscopic Sessile Droplets. *Soft Matter* **2010**, *6*, 2591−2612.
(17) Hu, H.; Larson, R. G. Analysis of the Microfluid Flow in an Evaporating Sessile Droplet. *Langmuir* **2005**, *21*, 3963−3971.
(18) Taylor, M.; Urquhart, A. J.; Zelzer, M.; Davies, M. C.; Alexander, M. R. Picoliter Water Contact Angle Measurement on Polymers. *Langmuir* **2007**, *23*, 6875−6878.
(19) Furuta, T.; Sakai, M.; Isobe, T.; Nakajima, A. Evaporation Behavior of Microliter- and Sub-Nanoliter-Scale Water Droplets on Two Different Fluoroalkylsilane Coatings. *Langmuir* **2009**, *25*, 11998−12001.
(20) Arcamone, J.; Dujardin, E.; Rius, G.; Pérez-Murano, F.; Ondarçuhu, T. Evaporation of Femtoliter Sessile Droplets Monitored with Nanomechanical Mass Sensors. *J. Phys. Chem. B* **2007**, *111*, 13020−13027.
(21) Talbot, E. L.; Berson, A.; Brown, P. S.; Bain, C. D. Evaporation of Picoliter Droplets on Surfaces with a Range of Wettabilities and Thermal Conductivities. *Phys. Rev. E* **2012**, *85* (6), 061604.
(22) Grossier, R.; Hammadi, Z.; Morin, R.; Magnaldo, A.; Veesler, S. Generating Nanoliter to Femtoliter Microdroplets with Ease. *Appl. Phys. Lett.* **2011**, *98*, 091916−.
(23) Grossier, R.; Magnaldo, A.; Veesler, S. Ultra-Fast Crystallization Due to Confinement. *J. Cryst. Growth* **2010**, *312*, 487−489.
(24) Velazquez, J. A.; Hileman, O. E., Jr. Studies on Nucleation from Solution of Some Soluble Inorganic Salts. *Can. J. Chem.* **1970**, *48*, 2896−2899.
(25) Bempah, O. A.; Hileman, O. E., Jr. Mean Lifetime of an Embryo in the Homogeneous Nucleation from Solution of the Tetracyanoplatinates(II) of Barium, Calcium, and Magnesium. *Can. J. Chem.* **1973**, *51*, 3435−3442.
(26) Langer, H.; Offermann, H. On the Solubility of Sodium Chloride in Water. *J. Cryst. Growth* **1982**, *60*, 389−392.
(27) Grossier, R.; Veesler, S. Reaching one Single and Stable Critical Cluster through Finite Sized Systems. *Cryst. Growth Des.* **2009**, *9*, 1917−1922.
(28) Gaitzsch, F.; Gäbler, A.; Kraume, M. Analysis of Droplet Expulsion in Stagnant Single Water-in-Oil-in-Water Double Emulsion Globules. *Chem. Eng. Sci.* **2011**, *66*, 4663−4669.
(29) Duncan, P. B.; Needham, D. Microdroplet Dissolution into a Second-Phase Solvent Using a Micropipet Technique: Test of the Epstein−Plesset Model for an Aniline−Water System. *Langmuir* **2006**, *22*, 4190−4197.
(30) Talreja, S.; Kenis, P. J. A.; Zukoski, C. F. A Kinetic Model To Simulate Protein Crystal Growth in an Evaporation-Based Crystallization Platform. *Langmuir* **2007**, *23*, 4516−4522.
(31) Deegan, R. D. Pattern Formation in Drying Drops. *Phys. Rev. E* **2000**, *61*, 475−485.
(32) Mchale, G.; Aqil, S.; Shirtcliffe, N. J.; Newton, M. I.; Erbil, H. Y. Analysis of Droplet Evaporation on a Superhydrophobic Surface. *Langmuir* **2005**, *21*, 11053−11060.